Ester derivatives of salinomycin efficiently eliminate breast cancer cells *via* ER-stress-induced apoptosis

Dominika Kuran, Sylwia Flis, Michał Antoszczak, Marlena Piskorek, Adam Huczyński

PII: S0014-2999(20)30929-8

DOI: https://doi.org/10.1016/j.ejphar.2020.173824

Reference: EJP 173824

To appear in: *European Journal of Pharmacology*

Received Date: 21 August 2020

Revised Date: 13 December 2020

Accepted Date: 16 December 2020

Please cite this article as: Kuran, D., Flis, S., Antoszczak, M., Piskorek, M., Huczyński, A., Ester derivatives of salinomycin efficiently eliminate breast cancer cells *via* ER-stress-induced apoptosis , *European Journal of Pharmacology*, https://doi.org/10.1016/j.ejphar.2020.173824.

CRediT authorship contribution statement

Dominika Kuran: Experiments performing, data analysis, writing – part of the original draft.

Sylwia Flis: Design and performing of the experiments, data analysis, visualization, writing – original draft, writing – review and editing, funding acquisition.

Marlena Piskorek: Generation of the part of western blot results.

Michał Antoszczak: Investigation, writing – original draft, writing – review and editing, visualization, funding acquisition.

Adam Huczyński: Resources, writing – review and editing, conceptualization, funding acquisition, formal analysis, supervision.

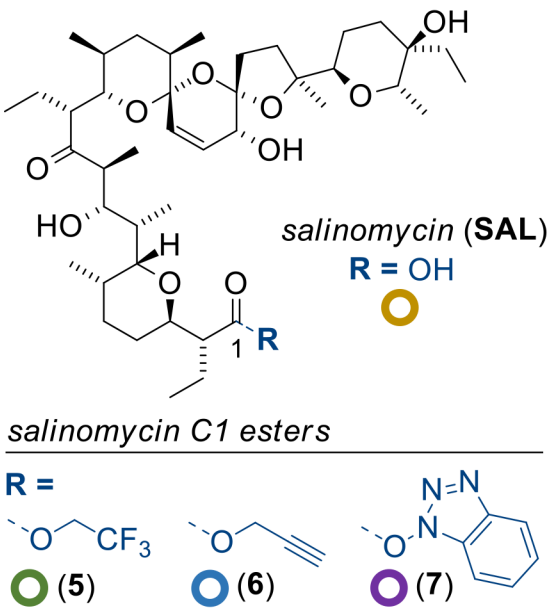

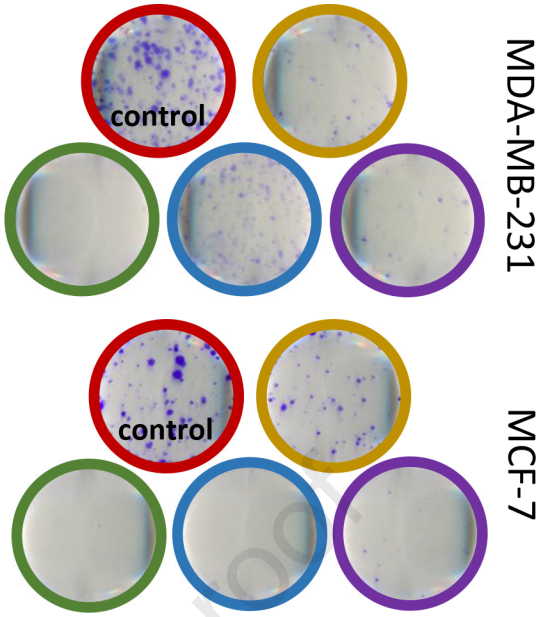

Ester derivatives of salinomycin efficiently eliminate breast cancer cells *via* ER-stress-induced apoptosis

Dominika Kuran[1], Sylwia Flis[1*], Michał Antoszczak[2], Marlena Piskorek[1], Adam Huczyński[2*]

[1]*Department of Pharmacology, National Medicines Institute, Chełmska 30/34, 00–725 Warsaw, Poland*
[2]*Department of Medical Chemistry, Faculty of Chemistry, Adam Mickiewicz University, Uniwersytetu Poznańskiego 8, 61–614 Poznań, Poland*

Abstract: The polyether ionophore salinomycin (**SAL**) has been found to selectively target breast cancer cells, including those with stem-like phenotype. On the other hand, **SAL** amides and esters obtained through derivatisation of the C1 carboxyl of the ionophore were found to exhibit anticancer properties, whilst reducing potential toxicity issues which often occur during standard chemotherapy. However, the studies on the activity and especially on the mechanisms of action of this class of semi-synthetic products against breast cancer cells are very limited. Therefore, in this work, we confirmed the anti-breast cancer activity of **SAL**, and further investigated the potential of its selected C1 amide and ester analogs to destroy breast cancer cells, including the highly aggressive triple-negative MDA-MB-231 cells. Importantly, **SAL** esters were found to be more potent than the native structure and their amide counterparts. Our data revealed that **SAL** ester derivatives, particularly compounds **5** and **7** (2,2,2-trifluoroethyl and benzotriazole ester of **SAL**, respectively), increase the level of p-eIF2α (Ser51) and IRE1α proteins. Additionally, an increased level of DNA damage indicators such as γH2AX protein and modified guanine (8-oxoG) was observed. These findings suggest that the apoptosis of MCF-7 and MDA-MB-231 cells induced by the most promising esters derived from **SAL** may result from the interaction between ER stress and DNA damage response mechanisms.

Key words: Breast adenocarcinoma; salinomycin; endoplasmic reticulum stress; DNA damage; apoptosis

*Correspondence: s.flis@nil.gov.pl (S.F.); adhucz@amu.edu.pl (A.H.)

1. Introduction

Breast cancer is the most frequent type of female cancer (Ataollahi et al., 2015), which is contracted by more than two million women each year throughout the world (World Health Organization – Cancer, 2020). Moreover, it causes the greatest number of cancer-related deaths among women (World Health Organization – Cancer, 2020; Shah et al., 2014), especially in the group of post-menopausal individuals (Akram et al., 2017). In the last decade, significant progress has been made to develop preventive methods and to understand breast cancer, which has resulted in more efficient, and less toxic treatment options for the disease (Sharma et al., 2010); the current ones involve a combination of various therapies, such as surgery, radiation, hormonal therapy, and/or chemotherapy. Within the large group of diverse breast cancers, various types could be identified on the basis of their invasiveness relative to that of the primary tumor sites (Feng et al., 2018), including triple-negative breast cancer (TNBC) with the poorest prognosis from among all breast cancer subtypes (Mehanna et al., 2019). TNBC makes up about 10–15% of all diagnosed breast cancers, and is characterized by a unique molecular profile, very aggressive nature, significant drug resistance, distinct metastatic patterns, and thus limited options of effective treatment (Aysola et al., 2013; Dawson et al., 2009). Therefore, although the mortality rate of breast cancer decreases due to widespread early screenings and advanced medical therapies (Sun et al., 2017), novel alternative methods with less adverse effects and a favorable risk-benefit ratio, particularly against TNBC variants, are much in demand.

Salinomycin (**SAL**, **1**, **Table 1**) is a naturally-occurring polyether ionophore first isolated from *Streptomyces albus*, which exhibits a very broad spectrum of bioactivities, including antibacterial, antiparasitic, antiviral, and also anticancer activity (Antoszczak, 2019a; Antoszczak and Huczyński, 2019; Miyazaki et al., 1974). The significant anticancer

properties of **SAL** were originally identified in the treatment of breast cancer in 2009, when it showed greater efficacy than the cytostatic drug taxol (paclitaxel) and nearly 16,000 other compounds used in the screening study, *i.a.* by selectively targeting a sub-population of breast cancer stem cells (CSCs) (Gupta et al., 2009). Of note, some preliminary clinical reports indicated that **SAL** is well-tolerated by cancer patients when used in appropriate doses (Naujokat and Steinhart, 2012). Several strategies have been developed to target specific biomarkers of TNBC or basal-like subtypes (Collignon et al., 2016; Penault-Llorca and Viale, 2012), and some of the promising therapeutic targets include the Wnt/β-catenin, Hedgehog and/or NOTCH signaling pathways (O'Toole et al., 2013). Thus, as the effects of several signal transduction pathways have been invoked to explain the change in phenotype composition after **SAL** treatment (Huang et al., 2018), extensive efforts have been made to explore the anticancer effects of **SAL** and its derivatives on breast cancer.

Indeed, as far as breast cancer is concerned, **SAL** was found to be able to induce growth inhibition, permanent cell cycle arrest, apoptosis and senescence of different human breast cancer cells, including TNBC variants. **SAL** could be also applied at a relatively low concentration for a longer time to overcome drug-resistance of breast cancer cells (Huang et al., 2018; Al Dhaheri et al., 2013). With respect to its semi-synthetic analogs, selected **SAL** amides and esters obtained by the chemical modification of the C1 carboxyl were more potent than the native structure in cell viability assays against primary acute lymphoblastic leukemia (ALL) cells (Antoszczak et al., 2018; Urbaniak et al., 2018), as well as identified as agents that may selectively overcome the resistance to platinum-based drugs in ovarian cancer (Michalak et al., 2020), which makes them promising candidates for the development of anticancer drug leads. However, although tertiary amides of **SAL** have been recently found to be more potent toward the MDA-MB-231 cell line than the parent structure

(Czerwonka et al., 2020), there are only limited studies on the effects of **SAL** secondary amides and its ester analogs against breast cancer cells, particularly toward highly aggressive variants. Furthermore, as the precise anticancer mechanism of action of **SAL** derivatives is not fully understood, intensive investigations in this direction are strongly recommended.

We therefore decided to characterize thoroughly the anticancer effects of **SAL** analogs obtained *via* derivatisation of the C1 carboxyl of the ionophore against breast cancer cells. Given the favorable anticancer potential of **SAL**, we examined the anti-breast cancer activity of its semi-synthetic derivatives selected from the group of the most promising C1 amides and esters (**Table 1**) (Antoszczak, 2019b). Along with the above studies, our aim was to unravel the mechanism of their anticancer action, with the hope of increasing the efficacy and reducing potential toxicity issues of the parent biomolecule.

2. Materials and methods

2.1. General procedures

All commercially available reagents and solvents were purchased from Merck (Germany) or Trimen Chemicals S.A. (Poland), and used in the experiments without further purification. Detailed description of the general procedures, equipment (NMR and mass spectrometers), measurement parameters, and software can be found in the Supplementary material.

2.2. Synthesis of salinomycin derivatives

Salinomycin (**SAL**) was prepared conveniently by isolation of its sodium salt from the commercially available veterinary premix SACOX®, followed by the acidic extraction, using the procedure described by us previously (Huczyński et al., 2012b). The synthesis of the six

SAL derivatives investigated in this study, *i.e.* three C1 amides **2**–**4** and three C1 esters **5**–**7** (**Table 1**), is also described elsewhere (Antoszczak et al., 2014a; Antoszczak et al., 2014b; Huczyński et al., 2012a; Huczyński et al., 2012b). The spectroscopic and spectrometric data of all these compounds were in good agreement with those found in the reference literature.

2.2.1. General procedure for preparation of salinomycin amides **2**–**4**

According to the reference procedures (Antoszczak et al., 2014a; Huczyński et al., 2012b), to a stirred solution of **SAL** (1.0 equiv.) in anhydrous CH_2Cl_2 at 0 °C, the following reagents were added: DCC (1.5 equiv.), HOBt hydrate (1.1 equiv., dissolved in anhydrous THF), and a respective amine (1.8 equiv.). The temperature of the reaction mixture was raised to room temperature, and stirring was continued for 24 h. Then, the solvents were evaporated under reduced pressure to dryness. The oily residue was suspended in CH_2Cl_2 and filtered off to remove the formed by-product (DCU). The filtrate was concentrated *in vacuo* and purified chromatographically on silica gel using the CombiFlash system to give the pure products **2**–**4** (59–88% yield) as clear oils. After thrice evaporation to dryness with *n*-pentane, the oily products were completely converted into white amorphous solids. The ^{1}H and ^{13}C NMR spectra of amides **2**–**4** can be found in the Supplementary material (Figs. S1–S6).

Propargyl amide of salinomycin **2***:* Yield: 138 mg, 88%. Isolated as a white amorphous solid, >95% pure by NMR and a single spot by TLC. Strains green with PMA; ^{1}H NMR (403 MHz, CD_2Cl_2) δ 7.07–6.98 (m, 1H), 6.11 (dd, *J* = 10.7, 2.2 Hz, 1H), 5.96 (dd, *J* = 10.7, 1.6 Hz, 1H), 4.36 (ddd, *J* = 17.6, 5.9, 2.5 Hz, 1H), 4.22 (ddd, *J* = 17.6, 5.3, 2.5 Hz, 1H), 4.13–4.05 (m, 1H), 4.01 (dt, *J* = 7.8, 1.9 Hz, 1H), 3.90 (ddd, *J* = 9.6, 5.9, 1.3 Hz, 1H), 3.87–3.76 (m, 2H), 3.73

(dd, *J* = 10.2, 2.6 Hz, 1H), 3.65 (ddd, *J* = 8.3, 5.3, 1.8 Hz, 2H), 2.97 (dq, *J* = 9.4, 7.4 Hz, 1H), 2.76–2.61 (m, 2H), 2.61–2.48 (m, 2H), 2.33 (dt, *J* = 12.6, 10.0 Hz, 1H), 2.22–2.10 (m, 2H), 2.05–0.50 (m, 52H) ppm; ^{13}C NMR (101 MHz, CD_2Cl_2) δ 213.0, 175.2, 133.8, 120.7, 106.7, 99.0, 89.1, 82.0, 80.0, 77.3, 75.6, 74.8, 71.3, 71.0, 69.7, 69.3, 67.3, 53.9, 48.0, 46.6, 40.7, 38.7, 37.1, 36.7, 33.0, 31.0, 30.6, 29.5, 28.9, 28.6, 26.9, 26.1, 22.5, 22.3, 20.5, 17.7, 17.3, 15.8, 15.0, 14.7, 14.2, 12.0, 11.4, 8.3, 6.5 ppm; ESI MS (*m/z*): $[M+Na]^+$ Calcd for $C_{45}H_{73}NNaO_{10}^+$ 810.5; Found 810.

4-fluorophenethyl amide of salinomycin **3***:* Yield: 143 mg, 82%. Isolated as a white amorphous solid, >95% pure by NMR and a single spot by TLC. UV-active and strains green with PMA; ^{1}H NMR (403 MHz, CD_2Cl_2) δ 7.36–7.27 (m, 2H), 7.01–6.92 (m, 2H), 6.52 (t, *J* = 5.8 Hz, 1H), 6.07 (dd, *J* = 10.7, 2.2 Hz, 1H), 5.95 (dd, *J* = 10.7, 1.5 Hz, 1H), 4.14 (ddd, *J* = 9.1, 6.7, 1.3 Hz, 1H), 4.01–3.96 (m, 1H), 3.89–3.74 (m, 3H), 3.74–3.50 (m, 5H), 3.00 (dq, *J* = 9.5, 7.3 Hz, 1H), 2.93 (d, *J* = 6.7 Hz, 1H), 2.87 (t, *J* = 7.6 Hz, 2H), 2.68–2.57 (m, 2H), 2.44 (s, 1H), 2.32 (dt, *J* = 12.6, 9.7 Hz, 1H), 2.22–2.13 (m, 1H), 2.05–0.50 (m, 52H) ppm; ^{13}C NMR (101 MHz, CD_2Cl_2) δ 213.9, 175.3, 163.0, 160.6, 136.00, 135.97, 133.8, 130.8, 130.7, 120.8, 115.3, 115.1, 106.8, 99.2, 88.7, 79.9, 77.4, 75.8, 74.6, 71.5, 71.0, 69.8, 67.6, 54.8, 49.0, 46.8, 41.2, 40.8, 38.9, 37.1, 36.7, 35.5, 33.3, 31.0, 30.6, 29.5, 28.7, 27.0, 26.0, 22.5, 21.0, 18.5, 17.5, 15.8, 14.9, 14.7, 13.9, 12.1, 11.8, 8.3, 6.5 ppm; ESI MS (*m/z*): $[M+Na]^+$ Calcd for $C_{50}H_{78}FNNaO_{10}^+$ 894.6; Found 894.9.

N-benzyl amide of salinomycin **4***:* Yield: 99 mg, 59%. Isolated as a white amorphous solid, >95% pure by NMR and a single spot by TLC. UV-active and strains green with PMA; ^{1}H NMR (403 MHz, CD_2Cl_2) δ 7.40–7.31 (m, 2H), 7.31–7.23 (m, 2H), 7.23–7.17 (m, 1H), 6.97–6.91 (m, 1H), 6.08 (dd, *J* = 10.7, 2.2 Hz, 1H), 5.93 (dd, *J* = 10.7, 1.5 Hz, 1H), 4.90 (dd, *J* = 15.3, 7.0 Hz, 1H), 4.60 (dd, *J* = 15.3, 4.9 Hz, 1H), 4.23–4.17 (m, 1H), 3.99–3.91 (m, 2H), 3.78 (d, *J* =

8.0 Hz, 1H), 3.72 (ddd, *J* = 10.0, 8.3, 4.5 Hz, 3H), 3.46 (dd, *J* = 12.1, 2.3 Hz, 1H), 2.99 (ddd, *J* = 14.7, 9.2, 7.3 Hz, 1H), 2.78–2.69 (m, 2H), 2.58 (dt, *J* = 8.4, 2.7 Hz, 1H), 2.44 (s, 1H), 2.27 (dt, *J* = 12.6, 9.9 Hz, 1H), 2.07 (ddd, *J* = 12.6, 9.8, 3.0 Hz, 1H), 2.00–0.50 (m, 52H) ppm; ^{13}C NMR (101 MHz, CD_2Cl_2) δ 213.4, 175.6, 140.6, 133.9, 128.5 (2C), 127.8 (2C), 127.0, 120.7, 106.7, 99.1, 88.9, 79.9, 77.2, 75.9, 74.6, 71.4, 70.9, 69.6, 67.4, 54.1, 48.6, 46.6, 43.0, 40.7, 38.8, 37.1, 36.8, 33.1, 31.0, 30.4, 29.6, 28.6, 27.0, 26.2, 22.4, 22.0, 20.7, 18.1, 17.5, 15.8, 14.9, 14.8, 14.3, 12.4, 11.5, 8.4, 6.5 ppm; ESI MS (*m/z*): $[M+Na]^+$ Calcd for $C_{49}H_{77}NNaO_{10}^+$ 862.5; Found 862.8.

2.2.2. Synthesis of 2,2,2-trifluoroethyl ester of salinomycin **5**

According to the reference procedure (Antoszczak et al., 2014b), to a stirred solution of **SAL** (500 mg, 0.66 mmol, 1.0 equiv.) in anhydrous CH_2Cl_2 the following reagents were added: DCC (206 mg, 1.00 mmol, 1.5 equiv.), PPy (50 mg, 0.34 mmol, 0.5 equiv.), 2,2,2-trifluoroethanol (500 mg, 5.00 mmol, 7.5 equiv.) and catalytic PTSA. The reaction mixture was first stirred at 0 °C for 6 h, and then for further 18 h at room temperature. The organic solvent was subsequently evaporated under reduced pressure to dryness. The residue was suspended in CH_2Cl_2 and filtered off to remove the formed by-product (DCU). Then, the filtrate was concentrated *in vacuo* and purified chromatographically on silica gel using the CombiFlash system to give the pure product **5** (71% yield) as a clear oil. After thrice evaporation to dryness with *n*-pentane, the oily product was completely converted into white amorphous solid. The ^{1}H and ^{13}C NMR spectra of ester **5** can be found in the Supplementary material (Figs. S7–S8).

Yield: 394 mg, 71%. Isolated as a white amorphous solid, >95% pure by NMR and a single spot by TLC. Strains green with PMA; ^{1}H NMR (400 MHz, C_6D_6) δ 6.12 (dd, *J* = 10.7, 1.5

Hz, 1H), 5.78 (dd, *J* = 10.7, 2.3 Hz, 1H), 5.25 (dq, *J* = 13.1, 8.9 Hz, 1H), 4.96 (dq, *J* = 13.1, 8.8 Hz, 1H), 4.31 (dd, *J* = 10.0, 5.7 Hz, 1H), 4.21 (dt, *J* = 9.1, 1.9 Hz, 1H), 4.14 (d, *J* = 9.1 Hz, 1H), 4.06 (dd, *J* = 10.9, 5.9 Hz, 1H), 3.85–3.72 (m, 2H), 3.69 (dd, *J* = 9.7, 2.3 Hz, 1H), 3.58 (dd, *J* = 10.3, 2.4 Hz, 1H), 3.12 (dq, *J* = 10.0, 7.2 Hz, 1H), 2.94 (td, *J* = 11.1, 4.0 Hz, 1H), 2.75 (d, *J* = 5.9 Hz, 1H), 2.62 (dt, *J* = 9.8, 2.6 Hz, 1H), 2.48 (dt, *J* = 13.4, 9.8 Hz, 1H), 2.35 (s, 1H), 2.24 (ddq, *J* = 14.4, 9.7, 7.2 Hz, 1H), 2.11–1.95 (m, 2H), 1.89 (ddd, *J* = 13.1, 6.7, 4.0 Hz, 1H), 1.80–0.50 (m, 49H) ppm; ^{13}C NMR (101 MHz, C_6D_6) δ 212.9, 172.9, 133.5, 120.5, 106.6, 98.9, 88.1, 79.3, 77.0, 74.05, 74.01, 71.8, 70.3, 69.1, 67.5, 60.8, 60.5, 55.3, 48.6, 47.0, 40.4, 38.4, 36.8, 36.6, 34.1, 32.8, 30.9, 30.3, 29.1, 28.1, 26.1, 25.8, 22.5, 22.4, 22.1, 19.6, 18.2, 17.2, 15.6, 14.3, 14.1, 13.9, 13.4, 11.4, 10.9, 7.7, 6.3 ppm, one signal overlapped; ESI MS (*m/z*): $[M+Na]^+$ Calcd for $C_{44}H_{71}F_3NaO_{11}^+$ 855.5; Found 855.

2.2.3. Synthesis of propargyl ester of salinomycin **6**

According to the reference procedure (Antoszczak et al., 2014b), a mixture of **SAL** (500 mg, 0.66 mmol, 1.0 equiv.), propargyl bromide (~80% in toluene; 171 mg, 1.45 mmol, 2.2 equiv.), DBU (173 mg, 1.15 mmol, 1.7 equiv.) and anhydrous toluene was heated at 90 °C for 5 h. After cooling, the mixture was concentrated *in vacuo* and purified chromatographically on silica gel using the CombiFlash system to give the pure product **6** (88% yield) as a clear oil. After thrice evaporation to dryness with *n*-pentane, the oily product was completely converted into a white amorphous solid. The ^{1}H and ^{13}C NMR spectra of ester **6** can be found in the Supplementary material (Figs. S9–S10).

Yield: 462 mg, 88%. Isolated as a white amorphous solid, >95% pure by NMR and a single spot by TLC. Strains green with PMA; ^{1}H NMR (400 MHz, C_6D_6) δ 6.13 (dd, *J* = 10.7, 1.3 Hz, 1H), 5.83 (dd, *J* = 10.8, 2.2 Hz, 1H), 5.36–5.20 (m, 2H), 4.41–4.32 (m, 1H), 4.26–4.12 (m,

2H), 4.08 (dd, *J* = 11.1, 6.0 Hz, 1H), 3.84–3.75 (m, 2H), 3.72 (dd, *J* = 9.7, 2.3 Hz, 1H), 3.64 (dd, *J* = 10.4, 2.4 Hz, 1H), 3.14 (dq, *J* = 10.1, 7.2 Hz, 1H), 3.00 (d, *J* = 5.4 Hz, 1H), 2.94 (td, *J* = 11.2, 4.1 Hz, 1H), 2.66 (dt, *J* = 9.7, 2.7 Hz, 1H), 2.55–2.43 (m, 1H), 2.28 (ddq, *J* = 14.4, 9.8, 7.2 Hz, 1H), 2.08 (d, *J* = 3.1 Hz, 1H), 2.05 (t, *J* = 2.5 Hz, 1H), 1.90 (dtd, *J* = 13.5, 6.7, 4.0 Hz, 1H), 1.80–0.50 (m, 51H) ppm; ^{13}C NMR (101 MHz, C_6D_6) δ 212.7, 173.9, 133.3, 120.7, 106.5, 99.0, 87.9, 79.0, 78.5, 77.0, 74.7, 74.3, 74.0, 71.7, 70.3, 69.2, 67.7, 55.9, 52.5, 48.5, 47.3, 40.5, 38.6, 36.8, 36.7, 33.1, 30.9, 30.3, 29.3, 28.1, 26.1, 25.8, 22.7, 22.1, 19.6, 18.4, 17.3, 15.6, 14.3, 14.1, 13.3, 11.6, 10.9, 7.6, 6.3 ppm; ESI MS (*m/z*): $[M+Na]^+$ Calcd for $C_{45}H_{72}NaO_{11}^+$ 811.5; Found 811.

2.2.4. Synthesis of benzotriazole ester of salinomycin **7**

According to the reference procedure (Huczyński et al., 2012a), a solution of **SAL** (1000 mg, 1.33 mmol, 1.0 equiv.) and DCC (418 mg, 2.03 mmol, 1.5 equiv.) in anhydrous CH_2Cl_2 as well as HOBt hydrate (197 mg, 1.46 mmol, 1.1 equiv.) dissolved in anhydrous THF were mixed, and stirred at 0 °C for 1 h. After this time, the reaction mixture was stirred at room temperature for 48 h. Then, the solvents were evaporated under reduced pressure to dryness. The oily residue was suspended in CH_2Cl_2 and filtered off to remove the formed by-product (DCU). The filtrate was concentrated *in vacuo* and purified chromatographically on silica gel using the CombiFlash system to give product **7** (45% yield) as a clear oil. After thrice evaporation to dryness with *n*-pentane, the oily product was completely converted into a white amorphous solid. Pure ester **7** was dissolved in warm ACN, and the solution was allowed to evaporate at room temperature. After several days, the crystals were formed in 30% yield. The ^{1}H and ^{13}C NMR spectra of ester **7** can be found in the Supplementary material (Figs. S11–S12).

Yield: 520 mg, 45%. Isolated as a white amorphous solid, >95% pure by NMR and a single spot by TLC. UV-active and strains green with PMA; ^{1}H NMR (600 MHz, CD_2Cl_2) δ 8.06–8.00 (m, 1H), 7.66–7.60 (m, 1H), 7.58–7.53 (m, 1H), 7.44–7.38 (m, 1H), 5.99 (dd, *J* = 10.7, 2.2 Hz, 1H), 5.88 (dd, *J* = 10.7, 1.2 Hz, 1H), 4.39–4.33 (m, 1H), 4.11 (ddd, *J* = 9.6, 4.8, 0.9 Hz, 1H), 3.95–3.90 (m, 1H), 3.87 (dd, *J* = 9.5, 2.3 Hz, 1H), 3.79–3.72 (m, 2H), 3.58–3.48 (m, 3H), 3.03 (dq, *J* = 9.3, 7.3 Hz, 1H), 2.77 (d, *J* = 4.4 Hz, 1H), 2.58 (dt, *J* = 10.2, 2.1 Hz, 1H), 2.46 (s, 1H), 2.27 (dt, *J* = 12.7, 9.7 Hz, 1H), 2.12 (ddd, *J* = 13.2, 9.9, 3.7 Hz, 1H), 2.07–1.98 (m, 1H), 1.97–0.50 (m, 51H) ppm; ^{13}C NMR (151 MHz, CD_2Cl_2) δ 213.0, 171.1, 143.8, 133.4, 129.2, 129.1, 125.0, 121.0, 120.4, 109.6, 106.7, 99.2, 88.4, 80.3, 77.5, 74.4 (2C), 72.9, 71.0, 69.8, 67.7, 55.5, 47.9, 46.8, 40.8, 39.0, 36.9, 36.5, 33.2, 31.1, 30.7, 29.4, 29.1, 26.8, 25.9, 23.0, 22.3, 20.9, 18.8, 17.4, 15.7, 14.8, 14.2, 13.5, 12.4, 11.8, 8.3, 6.5 ppm; ESI MS (*m/z*): $[M+Na]^+$ Calcd for $C_{48}H_{73}N_3NaO_{11}^+$ 890.5; Found 890.8.

2.3. Cell culture and agents treatment

Two human breast cancer cell lines, *i.e.* MCF-7 (human estrogen-dependent breast adenocarcinoma) and MDA-MB-231 (human estrogen-independent breast adenocarcinoma), were used in our studies, together with a normal human HMF cell line (normal breast fibroblasts). The cells were cultured in appropriate media such as RPMI 1640, Iscove's DMEM and MEME, respectively, containing additionally 10% fetal bovine serum (FBS, BioWest, Cytogen, Poland), 2 mM stabilized L-glutamine (BioWest) and antibiotics: 100 U/ml sodium penicillin, 100 μg/ml streptomycin and 250 ng/ml amphotericin B (Biowest). All cell types were incubated at 37 °C in a humidified atmosphere with 5% CO_2.

Tested compounds were dissolved in 100% dimethylsulfoxide (DMSO, Sigma-Aldrich, Poland), and then diluted in the media for experiments. The final concentration of DMSO, without affecting cell survival, was maintained at 0.2%.

2.4. MTT assay

The cells were seeded into 96-well plates at a density of 5×10^3 cells/well. After treatment with **SAL** and its six derivatives, 20 µl of 3-(4,5-dimethylthiazol-2-yl)-2,5-diphenyltetrazolium bromine (MTT) at the concentration of 5 mg/ml was added at 24, 48, and 72 h. Then, the cells were incubated for additional 4 h at 37 °C, and next, 180 µl of a solubilization solution (10% SDS) were added. The mixture was incubated at room temperature overnight. The product of solubilized formazan was spectrophotometrically quantified using a microtiter plate reader, Power Wave XS (Bio-Tek, Winooski, VT, USA), at 570 nm wavelength.

2.5. Oxidative DNA damage and cell cycle analysis

The cells (~1.5×10^5) were fixed with 1% paraformaldehyde on ice for 15 min and washed in phosphate buffered saline (PBS). Then, cells were permeabilinized in 0.1% PBS/Triton X-100 solution (PBST) for 30 min at room temperature and washed again in 0.01% PBST (230 × *g*, 5 min). Next, 100 µL of the diluted DNA/RNA damage antibody-FITC (StresMarq Biosciences Inc., Canada) were added to the cell pellet, and incubated for 1 h at room temperature in the dark. After cells washing (230 × *g*, 10 min), the pellet was re-suspended in propidium iodide (PI)/RNase staining solution (50 µg/ml PI, 100 µg/ml RNase in 0.1% PBST solution). The samples were characterized using a CyFlow Cube 8 (Sysmex,

Norderstedt, Germany) flow cytometer. The DNA histograms were analyzed using FCSExpress 5Flow software (De Novo Software, Glendale, CA, USA).

2.6. Analysis of apoptosis

Apoptosis was measured using annexin-V/fluorescein isothiocyanate (FITC) (BD Pharmingen, San Jose, California, USA). The staining procedure was conducted according to the manufacturer's instructions. The cells were harvested after treatment, washed twice with PBS, and then centrifuged. The cell pellet was resuspended in ice-cold binding buffer and annexin-V/FITC was added to the cell suspension. After 15 min of incubation in the dark at room temperature, the samples were analyzed using a flow cytometer.

Additionally, the cells were seeded into 12-well plates at a density of 7×10^4. Following exposure to the tested compounds, the cells were double-stained with fluorescein diacetate (FDA) and PI for 30 min at 37°C. Following two washing procedures in PBS, the culture medium without phenol red was added. The cell viability was observed under the *ZOE* Fluorescent Cell Imager microscope (Bio-Rad, Hercules, CA, USA).

2.7. Clonogenic assay

The cells (500/well) were seeded in 6-well plates and treated with **SAL** and its analogs (25 μM) for 24 h. Then, they were washed and allowed to grow for next 8–10 days in the growth media. The colonies were fixed with chilled methanol and stained with 0.5% crystal violet solution for 30 min. The visible colonies were manually calculated in triplicate, and images of the colonies were scanned.

2.8. Measurement of mitochondrial membrane potential ($\Delta\Psi_m$)

The mitochondrial membrane potential ($\Delta\Psi_m$) was measured by flow cytometry using MitoStatus Red (BD Pharmingen), a cationic lipophilic dye which accumulates within the mitochondria of healthy cells. The cells were stained according to the manufacturer's instructions and examined by flow cytometer. Additionally, the cells seeded into 12-well plates at a density of 7×10^4 were stained with MitoStatus Red according to the manufacturer's instructions, and examined by *ZOE* Fluorescent Cell Imager (Bio-Rad, Hercules, CA, USA).

2.9. Reactive oxygen species level analysis

The cells were incubated with redox-sensitive fluorochrome 2',7'-dichlorodihydrofluorescein diacetate (DCFDA) (Sigma-Aldrich) and analyzed using the CyFlow Cube 8 (Sysmex, Poland) to detect H_2O_2 and $^{\bullet}OH$ (Flis et al., 2019).

2.10. Immunoblotting

The cells were washed with cold PBS buffer and total proteins were extracted from the collected cells using RIPA buffer (25 mM Tris-HCl (pH 7.4), 150 mM NaCl, 0.1% SDS, 0.5% sodium deoxycholate, 1 mM EDTA, 1% NP-40) and protease inhibitors (Flis et al., 2019). The samples were fractionated on a 4%–20% TGX™ Precast Protein Gels (Bio-Rad, Poland). Next, the proteins were transferred onto a nitrocellulose membrane and probed with anti-human antibodies specific to PARP (#9542), caspase-3 (#9668), IRE1α (#3294), p-eIF2α (Ser51) (#3398), BiP (#3177), Ero1-Lα (#3264), p-p53 (Ser15) (#9286), p-Rb (Ser807/811) (#8516), γH2AX (#9718) and β-actin (#8457) (purchased from Cell Signaling Technologies, the Netherlands). The signals were detected using the enhanced chemiluminescence detection system (MicroChemi Bio-Imaging Systems, Israel).

2.11. Statistical analysis

The data are presented as mean values ± standard deviation (S.D.). Statistical comparisons between groups were performed by Student's *t*-test or one-way analysis of variance (ANOVA), followed by Student-Newman-Keuls *post-hoc* test. Significance was assumed at $P<0.05$ (marked with asterisks or crosses on graphs).

3. Results

3.1. Salinomycin ester derivatives inhibited cell viability

The first stage of the study was to assess the survival of MCF-7 and MDA-MB-231 breast cancer cells treated with salinomycin (**SAL**, **1**) and its derivatives (**2**–**7**) (**Table 1**) at three time intervals of 24, 48, and 72 h (**Fig. 1**). The tested compounds reduced the percentage of surviving cancer cells depending on the incubation time and dose used. Interestingly, both cancer cell lines showed a better response to ester derivatives (**5**–**7**) than to **SAL**, which was used as the reference compound. At a concentration of ≥25 μM and after 24 h of incubation, a decrease in cell survival by more than 70% was observed, and the changes in cancer cells survival induced by **SAL** derivatives, together with those of the unmodified ionophore, were statistically significant. Following 48 h and 72 h, the maximal inhibition of cell growth (90%, $P<0.01$) was observed for both cell types treated with products **5**–**7** at the concentration of ≥25 μM, whereas for **SAL** the same effect was observed at the concentration of 50 μM for MCF-7 and MDA-MB-231 after 48 h and 72 h, respectively. Our results clearly showed that MDA-MB-231 cells were less sensitive to **SAL** than MCF-7 cells. As to the amide analogs of **SAL**, only MDA-MB-231 cells were slightly more sensitive to the action of compounds **2** and **3** at the concentration of ≥50 μM and ≥25 μM, respectively,

and after 24 h treatment, in comparison to **SAL**. The viability of normal breast fibroblast cells treated with **SAL** and its C1 amide and ester analogs was also assessed under the same experimental conditions as for cancer cells (data not shown).

On the basis of the results obtained from MTT assay for all cell lines, the selectivity index (SI) indicating the selectivity of the tested compounds towards the cancer cells, was calculated according to the following formula: $SI = IC_{50(normal\ cells)}/IC_{50(cancer\ cells)}$. The values of the SI parameter depending on the time of incubation are collected in **Table 2**. The higher the SI ratio, the less specific a given compound is towards normal cells. In general, SI values >1.0 indicate some selectivity of the tested compounds, while values of SI >2.0 indicate highly selective compounds which can be supposed to be potentially safer therapeutic agents (Segun et al., 2019). However, according to the selectivity criteria, only **SAL** and three ester derivatives **5**, **6** and **7** could be considered as selective compounds against both MCF-7 and MDA-MB-231 breast cancer cells. Although for amides **2** and **4** also SI >1.0 when applied to MCF-7 cells, they precipitated in aqueous solution, therefore, only C1 ester derivatives were tested in the following studies. For further analysis, the tested compounds were used in the same concentration towards both cancer cell lines, and the established dose was that at which the lowest IC_{50} value was obtained for **SAL** against normal cells, *i.e.* ~25 µM.

3.2. Salinomycin ester derivatives inhibited breast cancer cell proliferation and induced cell apoptosis

One of the main indicators of cellular stress resulting from the activities of the tested compounds are changes in cell cycle progression. In this context, **Fig. 2A** shows changes in the percentage of cancer cells in particular phases of the cell cycle induced by the presence of the tested compound, depending on the type of the compound. **SAL** slightly induced the

accumulation of MCF-7 cells in G1 phase, whereas all ester derivatives (**5**–**7**) caused a significant increase in the number of cells in G1 phase, at the expense of S and G2/M phases. The observed effects were stronger for MDA-MB-231 cells; both **SAL** as well as its esters **5**–**7** caused the accumulation of cancer cells in G2/M phase with a simultaneous decrease in the number of cells in G1 and S phases. Moreover, pretreatment of MCF-7 and MDA-MB-231 cells with **SAL** and **5**–**7** gave not only a reduction in cell growth (in terms of cell division intensity), but also reduced reproductive ability of both breast cancer cell lines. While **SAL** induced the loss of colony-forming ability, its C1 ester derivatives, particularly compounds **5** and **7**, almost completely diminished the reproductive ability of MCF-7 and MDA-MB-231 cells (**Fig. 2B**).

As **SAL** was reported to mediate apoptosis in many human cancer cells, including breast cancer cells (Antoszczak, 2019a), we were interested to find whether the observed growth and cell viability inhibition upon the treatment with C1 ester derivatives were also associated with the induction of apoptosis. For this purpose, Annexin V/PI staining was performed, followed by flow cytometry. As shown in **Fig. 3A**, all ester derivatives effectively increased the percentage of apoptotic cells, and this process was time-dependent. After 48 h of incubation, the percentage of apoptotic cells was in the range of 45–90%. Surprisingly, the response of MDA-MB-231 cells to **SAL** treatment was even twice higher than that observed for the corresponding MCF-7 cells.

Microscopic examination also revealed significant changes in the cell morphology (**Fig. 3B**). The number of shrinking cells or cells with blebbing membranes was significantly increased in the **SAL** ester derivatives-treated group. The advanced level of apoptosis was also evidenced by a decrease in caspase-3 level, as well as an increase in γH2AX and poly(ADP-ribose)polymerase (PARP) protein cleavage. Interestingly, treatment of

MDA-MB-231 cells with the C1 ester derivatives caused a significant reduction of Rb phosphorylated at Ser807/811, whereas the changes in the level of p53 phosphorylated at Ser15 were the opposite in the tested cell lines (**Fig. 3C**). The latter observation is likely connected with the genetic status of the *TP53* gene, which is mutated in MDA-MB-231 cells.

3.3. Salinomycin ester derivatives induced changes in the mitochondrial membrane potential ($\Delta\Psi_m$)

To characterize the mechanism of apoptosis induced by **SAL** esters **5–7**, the mitochondrial membrane potential ($\Delta\Psi_m$) was measured by MitoStatus Red staining (**Fig. 4**). MCF-7 and MDA-MB-231 breast cancer cells revealed morphological changes after treatment with the tested compounds. The cells shrank and became loosely arranged, and additionally their adhesion was weakened. The intensity of fluorescence, measured with the use of a flow cytometer, decreased in MCF-7 cells especially after incubation with analogs **5–7** (**Figs. 4A** and **4B**). The observed effects were weaker for MDA-MB-231 cancer cells. A slight, but statistically significant, decrease in red fluorescence was detected after 48 h of incubation with compounds **5** and **7**. These results suggest that the evaluated C1 ester derivatives of **SAL** induce mitochondria-dependent apoptosis and the loss of $\Delta\Psi_m$ in MCF-7 cells is more potent than in the corresponding MDA-MB-231 cells.

3.4. Salinomycin ester derivatives induced changes in reactive oxygen species level, DNA damage and endoplasmic reticulum *(ER)-stress*

An important consequence of $\Delta\Psi_m$ disruption is the enhancement of oxidative stress. We found that changes in the reactive oxygen species level strongly depend on the type of compounds tested and the cancer cell lines used. A significantly elevated level of reactive

oxygen species was observed in MDA-MB-231 breast cancer cells after 24 h treatment with esters **5–7**, then the reactive oxygen species level was constant or slightly decreased after the next 24 h (**Fig. 5A**). Similar results were observed during the assessment of 8-oxoguanine (8-oxoG), an indicator of DNA damage caused by reactive oxygen species (**Fig. 5B**). Surprisingly, a reversed trend was found for MCF-7 cells, for which a decrease in reactive oxygen species levels was found to be compound-dependent. Even a four-time higher decrease in reactive oxygen species was observed for the MCF-7 cells treated with ester **7**, but only marginal changes in the level of 8-oxoG were detected for all compounds. Nevertheless, in both breast cancer cell lines, changes in the levels of proteins such as eIF2α phosphorylated at Ser51, BiP and Ero1-Lα were found (**Fig. 5C**). Additionally, IRE1α level, which reflects the activation of the IRE1α pathway (Deldicque et al., 2010), increased after the treatment with C1 ester derivatives when compared with control and **SAL** (**Fig. 5C**).

4. Discussion

Although many forms of treatment are available to patients affected by cancer, chemotherapy is still the most popular and effective option, however, very often it is burdened with unpleasant and serious side effects. Therefore, the search for new, highly bioactive compounds that could make the basis of better, more effective therapeutic strategies with fewer side effects is a top current interest. In this context, various studies have demonstrated that salinomycin (**SAL**) shows significant anticancer activity; its semi-synthetic analogs are thus the objects of intense research interest.

Following this lead, in our work, the anti-breast cancer effects of **SAL** and its analogs obtained *via* derivatisation of the C1 carboxyl of the ionophore were compared; the selected C1 ester derivatives of **SAL** were found to be the most promising candidates in this context.

Generally, both **SAL** and its esters reduced the population of breast cancer cells, but the effectiveness of the semi-synthetic products was higher than that of unmodified **SAL** on MCF-7 and MDA-MB-231 cells. The evaluated mechanism of action appeared to be not the same for all compounds tested as well as for all cell lines used. Nevertheless, **SAL** ester derivatives were found to inhibit the growth and viability of human breast cancer cells. Structural alterations, such as shrinkage and membrane fragmentation, were also observed after treatment with **SAL** analogs.

It is known that **SAL** as an ionophore can disrupt ionic homeostasis in cells, leading to an increase in intracellular levels of Ca^{2+} cations. The cells are most sensitive to depletion of extracellular Ca^{2+}, especially in G1 and at the G1/S and G2/M transitions (Roderick and Cook, 2008). We observed cell cycle arrest in G1 and G2/M phases in MCF-7 and MDA-MB-231 cells, respectively. The Rb and p53 proteins, which act as tumor suppressors, are key regulators of cell proliferation by controlling progression through the restriction points of the cell cycle. Treatment of the cells with the evaluated compounds resulted in the abrogation of Rb phosphorylation at Ser807/811, and as a consequence, the cell cycle arrest. Additionally, an increased level of p53 phosphorylation at Ser15 was observed in MCF-7 cells. Phosphorylation of p53 at this site is crucial for its stabilization and is essential for the induction of cell cycle arrest. However, in response to severe DNA damage and/or ER stress, p53 induces apoptosis (Lin et al., 2012; Zhao et al., 2008). With respect to the MDA-MB-231 cells, inhibition of cell cycle progression in the G2/M phase is p53-independent, and may be due to alterations in other components in the pathway controlling this checkpoint.

Generally, apoptosis may be induced either by sustained Ca^{2+} influx *via* activated channels or by the release of calcium by a stressed endoplasmic reticulum (ER) (Kaushik et al., 2018). The latter phenomenon seems to be responsible for the induction of apoptosis in

our study. As a response to prolonged ER stress conditions, the unfolded protein response (UPR) signal transduction cascade is directly activated to counteract the occurring damage, but when ER stress is not reduced/softened, the UPR triggers apoptosis (Siwecka et al., 2019). We observed an increased level of IRE1α protein, the one from three main sensor proteins that recognize ER stress, in breast cancer cells after treatment with C1 ester analogs of **SAL**. Upon accumulation of misfolded proteins in ER, BiP protein, the main ER stress marker, gets released and allows oligomerization of IRE1α and protein kinase-like ER kinase (PERK). The western blot analysis of UPR-associated proteins revealed that the levels of BiP and Ero1-Lα (especially in MCF-7 cells) were increased after treatment with C1 esters of **SAL**. On the other hand, the level of pospho-eIF2α (Ser51) protein, the main downstream effector of the PERK-dependent UPR signaling pathway (the second sensor protein), was also increased after treatment with C1 ester analogs in MDA-MB-231 cells, and to a much lesser degree in MCF-7 cells. However, the level of phosho-eIF2α was strongly elevated in both breast cancer cell lines treated with **SAL**. Similar results have been obtained recently by Zhang et al. (2019) who showed that **SAL** treatment triggered ER stress by the PERK sensor in PC-3 prostate cancer cells.

The final result of the treatment of evaluated cell lines with **SAL** ester derivatives, especially compounds **5** and **7**, was the induction of cell death confirmed by flow cytometry analysis using annexin V/PI staining. The advanced level of apoptosis was also demonstrated by a decrease in the level of caspase-3, a cysteine protease belonging to the group of executive caspases degrading cellular proteins, indirectly contributing to the degradation of genetic material as well as PARP protein, which plays an important role in the DNA repair processes; its proteolytic degradation was also confirmed.

Of note is that the **SAL** C1 ester derivatives induced mitochondrial dysfunction, especially in MCF-7 breast cancer cells. Often, an important consequence of disruption of the $\Delta\Psi_m$ is an increment in oxidative stress. With respect to the MCF-7 cells, the decrease in mitochondrial potential was accompanied by a decrease in the level of reactive oxygen species and oxidative DNA damage (measured by 8-oxoG, the indicator of oxidative DNA damage). The changes in the mitochondrial potential were not highlighted very well in the corresponding MDA-MB-231 cells (except for unmodified **SAL**), although the concomitant increase in the reactive oxygen species and 8-oxoG levels were observed. These observations agree with the concept that higher (more polarized) $\Delta\Psi_m$ is associated with greater reactive oxygen species production by mitochondria (Li et al., 2013). Nevertheless, both mechanisms can be beneficial in the treatment strategy of cancer patients.

A characteristic feature of cancer cells is the generation of high levels of reactive oxygen species and the accumulation of genomic mutations under increased oxidative stress. Therefore, lowering the reactive oxygen species level in cancer cells may be associated with the inhibition of genetic instability and disease progress. On the other hand, pro-oxidizing agents, such as **SAL** (Managò et al., 2015) and its derivatives, may in some circumstances raise the level of reactive oxygen species in cancer cells above the tolerated threshold. A consequence is the generation of DNA lesions because of an 8-oxoG production (as a result of guanine oxidation). Insertion of 8-oxoG during replication generates DNA double-strand breaks (DSBs), which affects genome integrity and can activate cell death processes. The results that have been obtained by Tyagi and Patro (2019) showed an approximately 1.5-fold increase in γH2AX in MCF-7^{DDP} cells (cisplatin-resistant variant) after 24 h of treatment with **SAL**. We also observed an elevated level of γH2AX after treatment with **SAL**, but importantly, this effect was more enhanced in the cells treated with the C1

ester derivatives of the ionophore. Often, γH2AX is considered only as a DSBs marker, but it should be noticed that it can also play a pivotal role during apoptosis, as one of the factors involved in apoptotic DNA fragmentation.

5. Conclusions

To sum up, our studies clearly confirmed the findings of other authors demonstrating significant anti-breast cancer effects of salinomycin (**SAL**). Furthermore, we also identified a cohort of promising **SAL** derivatives with enhanced activity against breast cancer cells. Of note is that the breast cancer cells demonstrated increased sensitivity to the action of compounds derived from **SAL** when compared to normal mammary fibroblasts. Moreover, our results showed that the ester analogs obtained through derivatisation of the C1 carboxyl of **SAL**, especially compounds **5** and **7** (2,2,2-trifluoroethyl and benzotriazole ester of **SAL**, respectively), exhibit a more efficient ability to eliminate triple-negative breast cancer (TNBC) cells (MDA-MB-231 cell line) than both the unmodified **SAL** and its C1 amide counterparts. This observation is essential, because TNBC is an aggressive form of breast cancer with limited treatment options. On the other hand, there was no denial regarding the different response (signaling) across the two breast cancer cell lines, and it was independent from the rate of death; it may be explained by the mutational background of the cell lines. In this context, **SAL** derivatives, like ester **7**, may be beneficial if treatment is given based on genetic status (targeted approach).

The chemical modification of **SAL** biomolecule seems to be thus an extremely interesting direction of research, as it may lead to the discovery of candidates for new anticancer agents. Our results showed that **SAL** esters **5** and **7** should be recognized as the lead structures for further investigation, including *in vivo* studies.

Acknowledgements

The research was financed from the statutory activity of the National Medicines Institute. M.A. wishes to acknowledge the Polish Science Centre (NCN) for financial support by a grant SONATA (2016/23/D/ST5/00242). M.A. wishes also to acknowledge the NCN and the Polish National Agency for Academic Exchange (NAWA) for the scholarships under the UWERTURA (2019/32/U/ST4/00092) and the BEKKER programme (PPN/BEK/2019/1/00034), respectively, and the Polish Ministry of Science and Higher Education (MNiSW) for the scholarship for outstanding young scientists in the years 2020–2023 (STYP/15/1665/E-336/2020).

CRediT authorship contribution statement

Dominika Kuran: Experiments performing, data analysis, writing – part of the original draft.

Sylwia Flis: Design and performing of the experiments, data analysis, visualization, writing – original draft, writing – review and editing, funding acquisition.

Michał Antoszczak: Investigation, writing – original draft, writing – review and editing, visualization, funding acquisition.

Marlena Piskorek: Generation of the part of western blot results.

Adam Huczyński: Resources, writing – review and editing, conceptualization, funding acquisition, formal analysis, supervision.

Declaration of competing interests

The authors declare that they have no known competing financial interests or personal relationships that could have appeared to influence the work reported in this paper.

References

Akram, M., Iqbal, M., Daniyal, M., Khan, A.U., 2017. Awareness and current knowledge of breast cancer. Biol. Res. 50, 33. https://doi.org/10.1186/s40659-017-0140-9.

Al Dhaheri, Y., Attoub, S., Arafat, K., AbuQamar, S., Eid, A., Al Faresi, N., Iratni, R., 2013. Salinomycin induces apoptosis and senescence in breast cancer: Upregulation of p21, downregulation of survivin and histone H3 and H4 hyperacetylation. Biochim. Biophys. Acta 1830, 3121–3135. https://doi.org/10.1016/j.bbagen.2013.01.010.

Antoszczak, M., 2019a. A medicinal chemistry perspective on salinomycin as a potent anticancer and anti-CSCs agent. Eur. J. Med. Chem. 164, 366–377. https://doi.org/10.1016/j.ejmech.2018.12.057.

Antoszczak, M., 2019b. A comprehensive review of salinomycin derivatives as potent anticancer and anti-CSCs agents. Eur. J. Med. Chem. 166, 48–64. https://doi.org/10.1016/j.ejmech.2019.01.034.

Antoszczak, M., Huczyński, A., 2019. Salinomycin and its derivatives – A new class of multiple-targeted "magic bullets". Eur. J. Med. Chem. 176, 208–227. https://doi.org/10.1016/j.ejmech.2019.05.031.

Antoszczak, M., Maj, E., Stefańska, J., Wietrzyk, J., Janczak, J., Brzezinski, B., Huczyński, A., 2014a. Synthesis, antiproliferative and antibacterial activity of new amides of salinomycin. Bioorg. Med. Chem. Lett. 24, 1724–1729. https://doi.org/10.1016/j.bmcl.2014.02.042.

Antoszczak, M., Popiel, K., Stefańska, J., Wietrzyk, J., Maj, E., Janczak, J., Michalska, G., Brzezinski, B., Huczyński, A., 2014b. Synthesis, cytotoxicity and antibacterial activity of new esters of

polyether antibiotic-salinomycin. Eur. J. Med. Chem. 76, 435–444. https://doi.org/10.1016/j.ejmech.2014.02.031.

Antoszczak, M., Urbaniak, A., Delgado, M., Maj, E., Borgström, B., Wietrzyk, J., Huczyński, A., Yuan, Y., Chambers, T.C., Strand, D., 2018. Biological activity of doubly modified salinomycin analogs – Evaluation *in vitro* and *ex vivo*. Eur. J. Med. Chem. 156, 510–523. https://doi.org/10.1016/j.ejmech.2018.07.021.

Ataollahi, M.R., Sharifi, J., Paknahad, M.R., Paknahad, A., 2015. Breast cancer and associated factors: A review. J. Med. Life 8, 6–11.

Aysola, K., Desai, A., Welch, C., Xu, J., Qin, Y., Reddy, V., Matthews, R., Owens, C., Okoli, J., Beech, D.J., Piyathilake, C.J., Reddy, S.P., Rao, V.N., 2013. Triple negative breast cancer – An overview. Hereditary Genet. 2013, pii: 001. https://doi.org/10.4172/2161-1041.S2-001.

Collignon, J., Lousberg, L., Schroeder, H., Jerusalem, G., 2016. Triple-negative breast cancer: Treatment challenges and solutions. Breast Cancer (Dove Med. Press) 8, 93–107. https://doi.org/10.2147/BCTT.S69488.

Czerwonka, D., Urbaniak, A., Sobczak, S., Piña-Oviedo, S., Chambers, T.C., Antoszczak, M., Huczyński, A., 2020. Synthesis and anticancer activity of tertiary amides of salinomycin and their C20-oxo analogues. ChemMedChem 15, 236. https://doi.org/10.1002/cmdc.201900593.

Dawson, S.J., Provenzano, E., Caldas, C., 2009. Triple negative breast cancers: Clinical and prognostic implications. Eur. J. Cancer 45, 27–40. https://doi.org/10.1016/S0959-8049(09)70013-9.

Deldicque, L., Cani, P.D., Philp, A., Raymackers, J.M., Meakin, P.J., Ashford, M.L.J., Delzenne, N.M., Francaux, M., Baar, K., 2010. The unfolded protein response is activated in skeletal muscle by high-fat feeding: Potential role in the downregulation of protein synthesis. Am. J. Physiol. Endocrinol. Metab. 299, E695–E705. https://doi.org/10.1152/ajpendo.00038.2010.

Feng, Y., Spezia, M., Huang, S., Yuan, C., Zeng, Z., Zhang, L., Ji, X., Liu, W., Huang, B., Luo, W., Liu, B., Lei, Y., Du, S., Vuppalapati, A., Luu, H.H., Haydon, R.C., He, T.C., Ren, G., 2018. Breast cancer development and progression: Risk factors, cancer stem cells, signaling pathways, genomics,

and molecular pathogenesis. Genes Dis. 5, 77–106. https://doi.org/10.1016/j.gendis.2018.05.001.

Flis, S., Bratek, E., Chojnacki, T., Piskorek, M., Skorski, T., 2019. Simultaneous inhibition of BCR-ABL1 tyrosine kinase and PAK1/2 serine/threonine kinase exerts synergistic effect against chronic myeloid leukemia cells. Cancers (Basel) 11, 1544. https://doi.org/10.3390/cancers11101544.

Gupta, P.B., Onder, T.T., Jiang, G., Tao, K., Kuperwasser, C., Weinberg, R.A., Lander, E.S., 2009. Identification of selective inhibitors of cancer stem cells by high-throughput screening. Cell 138, 645–659. https://doi.org/10.1016/j.cell.2009.06.034.

Huang, X., Borgström, B., Stegmayr, J., Abassi, Y., Kruszyk, M., Leffler, H., Persson, L., Albinsson, S., Massoumi, R., Scheblykin, I.G., Hegardt, C., Oredsson, S., Strand, D., 2018. The molecular basis for inhibition of stemlike cancer cells by salinomycin. ACS Cent. Sci. 4, 760–767. https://doi.org/10.1021/acscentsci.8b00257.

Huczyński, A., Janczak, J., Antoszczak, M., Stefańska, J., Brzezinski, B., 2012a. X-ray, FT-IR, NMR and PM5 structural studies and antibacterial activity of unexpectedly stable salinomycin-benzotriazole intermediate ester. J. Mol. Struct. 1022, 197–203. https://doi.org/10.1016/j.molstruc.2012.05.019.

Huczyński, A., Janczak, J., Stefańska, J., Antoszczak, M., Brzezinski, B., 2012b. Synthesis and antimicrobial activity of amide derivatives of polyether antibiotic – salinomycin. Bioorg. Med. Chem. Lett. 22, 4697–4702. https://doi.org/10.1016/j.bmcl.2012.05.081.

Kaushik, V., Yakisich, J.S., Kumar, A., Azad, N., Iyer, A.K.V., 2018. Ionophores: Potential use as anticancer drugs and chemosensitizers. Cancers (Basel) 10, 360. https://doi.org/10.3390/cancers10100360.

Li, X., Fang, P., Mai, J., Choi, E.T., Wang, H., Yang, X.F., 2013. Targeting mitochondrial reactive oxygen species as novel therapy for inflammatory diseases and cancers. J. Hematol. Oncol. 6, 19. https://doi.org/10.1186/1756-8722-6-19.

Lin, W.C., Chuang, Y.C., Chang, Y.S., Lin, W.C., Chuang, Y.C., Chang, Y.S., Lai, M.D., Teng, Y.N., Su, I.J., Wang, C.C., Lee, K.H., Hung, J.H., 2012. Endoplasmic reticulum stress stimulates p53 expression through NF-κB activation. PLoS One. 7, e39120. https://doi.org/10.1371/journal.pone.0039120.

Managò, A., Leanza, L., Carraretto, L., Sassi, N., Grancara, S., Quintana-Cabrera, R., Trimarco, V., Toninello, A., Scorrano, L., Trentin, L., Semenzato, G., Gulbins, E., Zoratti, M., Szabò, I., 2015. Early effects of the antineoplastic agent salinomycin on mitochondrial function. Cell Death Dis. 6, e1930. https://doi.org/10.1038/cddis.2015.263.

Mehanna, J., Haddad, F.G.H., Eid, R., Lambertini, M., Kourie, H.R., 2019. Triple-negative breast cancer: Current perspective on the evolving therapeutic landscape. Int. J. Womens Health 11, 431–437. https://doi.org/10.2147/IJWH.S178349.

Michalak, M., Lach, M.S., Antoszczak, M., Huczyński, A., Suchorska, W.M., 2020. Overcoming resistance to platinum-based drugs in ovarian cancer by salinomycin and its derivatives – An *in vitro* study. Molecules 25, 537. https://doi.org/10.3390/molecules25030537.

Miyazaki, Y., Shibuya, M., Sugawara, H., Kawaguchi, O., Hirsoe, C., 1974. Salinomycin, a new polyether antibiotic. J. Antibiot. (Tokyo) 27, 814–821. https://doi.org/10.7164/antibiotics.27.814.

Naujokat, C., Steinhart, R., 2012. Salinomycin as a drug for targeting human cancer stem cells. J. Biomed. Biotechnol. 2012, 950658. https://doi.org/10.1155/2012/950658.

O'Toole, S.A., Beith, J.M., Millar, E.K., West, R., McLean, A., Cazet, A., Swarbrick, A., Oakes, S.R., 2013. Therapeutic targets in triple negative breast cancer. J. Clin. Pathol. 66, 530–542. https://doi.org/10.1136/jclinpath-2012-201361.

Penault-Llorca, F., Viale, G., 2012. Pathological and molecular diagnosis of triple-negative breast cancer: A clinical perspective. Ann. Oncol. 23, 19–22. https://doi.org/10.1093/annonc/mds190.

Roderick, H.L., Cook, S.J., 2008. Ca^{2+} signalling checkpoints in cancer: Remodelling Ca^{2+} for cancer cell proliferation and survival. Nat. Rev. Cancer. 8, 361–375. https://doi.org/10.1038/nrc2374.

Segun, P.A., Ogbole, O.O., Ismail, F.M.D., Nahar, L., Evans, A.R., Ajaiyeoba, E.O., Sarker, S.D., 2019. Resveratrol derivatives from *Commiphora africana* (A. Rich.) Endl. display cytotoxicity and selectivity against several human cancer cell lines. Phytother. Res. 33, 159–166. https://doi.org/10.1002/ptr.6209.

Shah, R., Rosso, K., Nathanson, S.D., 2014. Pathogenesis, prevention, diagnosis and treatment of breast cancer. World J. Clin. Oncol. 5, 283–298. https://doi.org/10.5306/wjco.v5.i3.283.

Sharma, G.N., Dave, R., Sanadya, J., Sharma, P., Sharma, K.K., 2010. Various types and management of breast cancer: An overview. J. Adv. Pharm. Technol. Res. 1, 109–126.

Siwecka, N., Rozpędek, W., Pytel, D., Wawrzynkiewicz, A., Dziki, A., Dziki, Ł., Diehl, J.A., Majsterek, I., 2019. Dual role of endoplasmic reticulum stress-mediated unfolded protein response signaling pathway in carcinogenesis. Int. J. Mol. Sci. 20, 4354. https://doi.org/10.3390/ijms20184354.

Sun, Y.S., Zhao, Z., Yang, Z.N., Xu, F., Lu, H.J., Zhu, Z.Y., Shi, W., Jiang, J., Yao, P.P., Zhu, H.P., 2017. Risk factors and preventions of breast cancer. Int. J. Biol. Sci. 13, 1387–1397. https://doi.org/10.7150/ijbs.21635.

Tyagi, M., Patro, B.S., 2019. Salinomycin reduces growth, proliferation and metastasis of cisplatin resistant breast cancer cells *via* NF-κB deregulation. Toxicol. In Vitro 60, 125–133. https://doi.org/10.1016/j.tiv.2019.05.004.

Urbaniak, A., Delgado, M., Antoszczak, M., Huczyński, A., Chambers, T.C., 2018. Salinomycin derivatives exhibit activity against primary acute lymphoblastic leukemia (ALL) cells *in vitro*. Biomed. Pharmacother. 99, 384–390. https://doi.org/10.1016/j.biopha.2018.01.081.

World Health Organization – Cancer. https://www.who.int/cancer/en/ (accessed 20 July 2020).

Zhang, Y., Li, F., Liu, L., Jiang, H., Hu, H., Du, X., Ge, X., Cao, J., Wang, Y., 2019. Salinomycin triggers endoplasmic reticulum stress through ATP2A3 upregulation in PC-3 cells. BMC Cancer 19, 381. https://doi.org/10.1186/s12885-019-5590-8.

Zhao, H., Traganos, F., Darzynkiewic, Z., 2008. Phosphorylation of p53 on Ser15 during cell cycle caused by Topo I and Topo II inhibitors in relation to ATM and Chk2 activation. Cell Cycle. 7, 3048–3055. https://doi.org/10.4161/cc.7.19.6750.

Table 1. Structure of salinomycin (**SAL**, **1**) and its derivatives (**2**–**7**) studied in this work.

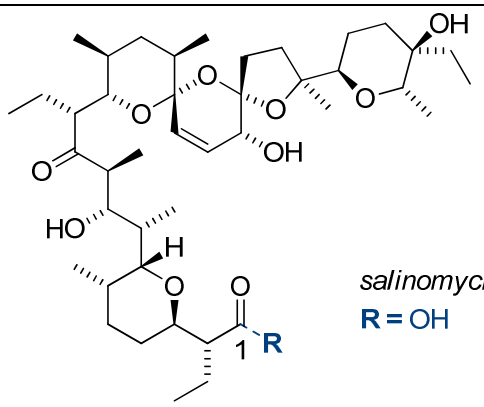

salinomycin (**SAL**, **1**)
R = OH

Amide series		Ester series	
No.	**R =**	**No.**	**R =**
2		**5**	
3	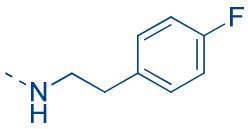	**6**	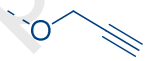
4		**7**	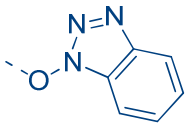

Table 2. The IC_{50} and selectivity indexes (SI) values of HMF, MCF-7 and MDA-MB-231 after 48 h incubation with salinomycin (**SAL**, **1**) and its analogs (**2**–**7**).

		IC50 [μM]		**SI ($IC50_{normal\ cells}/IC50_{cancer\ cells}$)**	
Compound	**HMF**	**MCF-7**	**MDA-MB-231**	**HMF/MCF-7**	**HMF/ MDA-MB-231**
1 (SAL)	26	27	14	1.0	**1.9**
2	20	16.7	28.4	**1.2**	0.7
3	11	18.9	15	0.6	0.7
4	4.8	2.8	16.1	**1.7**	0.3
5	18.5	15.3	4.5	**1.2**	**4.1**
6	12.2	12.6	10.4	1.0	**1.2**
7	12.5	4.1	2.6	**3.0**	**4.8**

FIGURE LEGENDS

Fig. 1. Effect of salinomycin amide (2–4) and ester derivatives (5–7) on cell viability of MCF-7 and MDA-MB-231 breast cancer cell lines. The cells were treated for 24, 48 and 72 h with the indicated doses of compounds followed by MTT assay. Each point represents the mean ± S.D. (n≥5), $^{\#}P$<0.002 in comparison with salinomycin (**SAL**).

Fig. 2. Salinomycin ester derivatives (5–7) inhibit growth of MCF-7 and MDA-MB-231 cells. A. Changes in cell cycle distribution of MCF-7 and MDA-MB-231 cells after treatment with the indicated compounds (25 μM). Each bar represents the mean ± S.D. (n≥3). A significant difference compared with **SAL** at P≤0.05 is indicated by an asterisk (*). Representative histograms from flow cytometry analysis are shown in the Supplementary material (Fig. S13). **B.** Clonogenic assay. The cells (500/well) after 24 h treatment with salinomycin (**SAL**) and its ester derivatives (**5–7**) were grown for up to 10 days in the growth medium. Colonies were visualized by 0.5% crystal violet staining and photographed.

Fig. 3. Ester derivatives (5-7) effectively induce apoptosis in MCF-7 and MDA-MB-231 cells. A. Detection of apoptosis by using the Annexin V-fluorescein isothiocyanate (FITC)/propidium iodide (PI) staining. Data are expressed as mean ± S.D. (n≥4); *P≤0.01 in comparison to control cells; $^{\#}P$≤0.04 in comparison to salinomycin (**SAL**). **B.** Representative microphotographs present live-dead staining using FDA and PI 24 h post treatment with 25 μM of the evaluated compounds. Cells were visualized under a fluorescent microscope *ZOE* Fluorescent Cell Imager, magnification 50–80×, scale bar 60–100 μm. Green fluorescence – live cells, red fluorescence – dead cells. **C.** Representative western blots analysis of the indicated proteins. β-actin was used as a loading control. All evaluated compounds were tested at the concentration of 25 μM.

Fig. 4. Changes in mitochondrial membrane potential. A. Histograms representing the geometric mean fluorescence intensity (MFI) of MitoStatus Red ± S.D. (n≥4), *P<0.04 in comparison to control, $^{\#}P$<0.03 in comparison to salinomycin (**SAL**). **B.** Representative microphotographs present MCF-7 cells treated for 24 h with **SAL** and its ester derivatives (**5–7**). A decrease in red fluorescence intensity reflects loss of mitochondrial membrane potential visualized under the fluorescent microscope *ZOE* Fluorescent Cell Imager, magnification 40×, scale bar 50 μm. All evaluated compounds were tested at the concentration of 25 μM.

Fig. 5. Analysis of intracellular reactive oxygen species level. A. Histograms representing the MFI of DCFDA ± S.D. (n≥4), *P≤0.01 in comparison to control, $^{\#}P$<0.03 in comparison to salinomycin (**SAL**). Representative histograms from flow cytometry analysis are shown in the

Supplementary material (Fig. S14, left panel) **B.** Oxidative DNA damage analysis. Mean of 8-oxoguanine (8-oxoG) fluorescence ± S.D. (n≥3), **P*<0.04 in comparison to control, $^{\#}$*P*<0.03 in comparison to **SAL**. Representative histograms from flow cytometry analysis are shown in the Supplementary material (Fig. S14, right panel). **C.** Representative western blot analysis of the indicated proteins. β-actin was used as a loading control. All evaluated compounds were tested at the concentration of 25 μM.

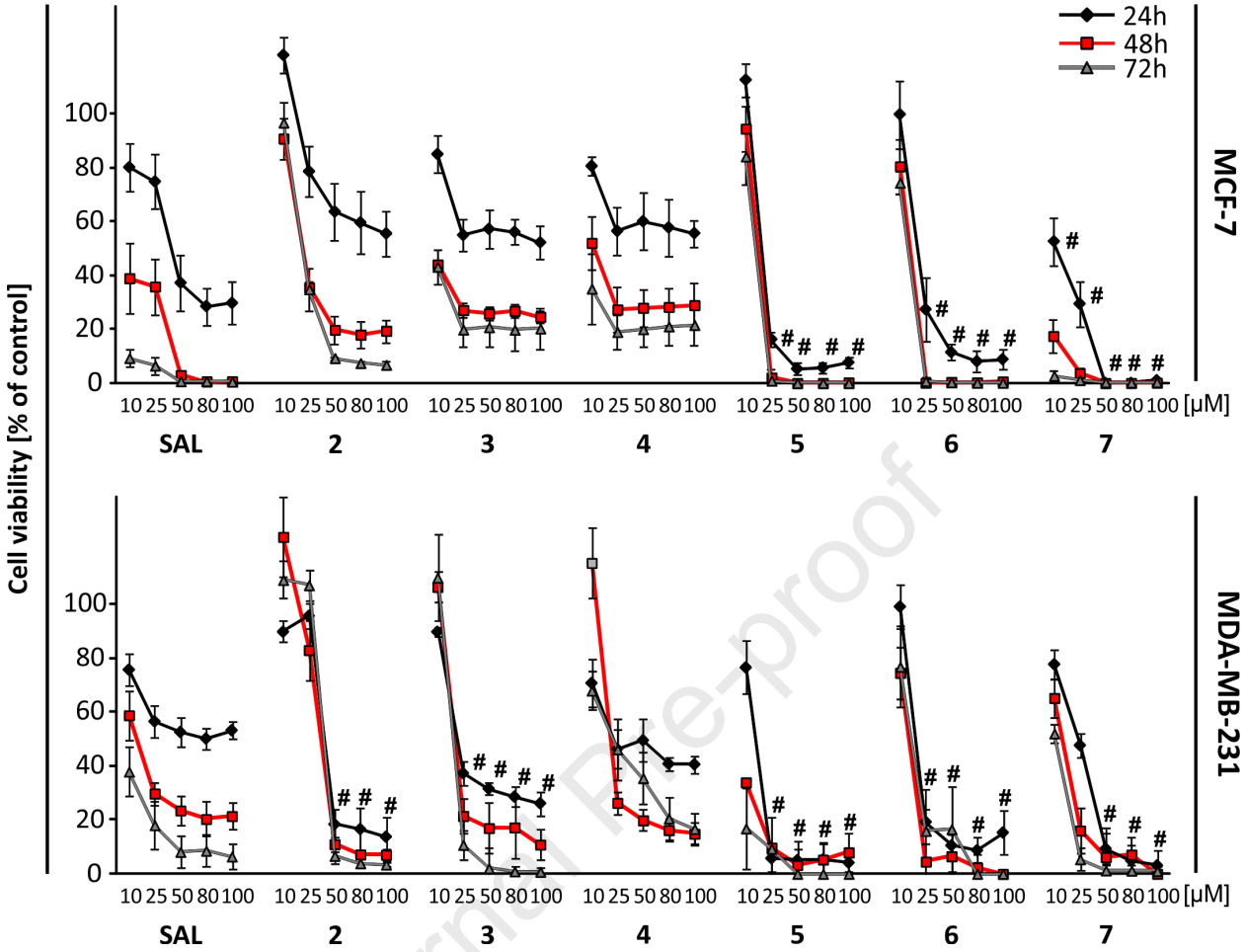

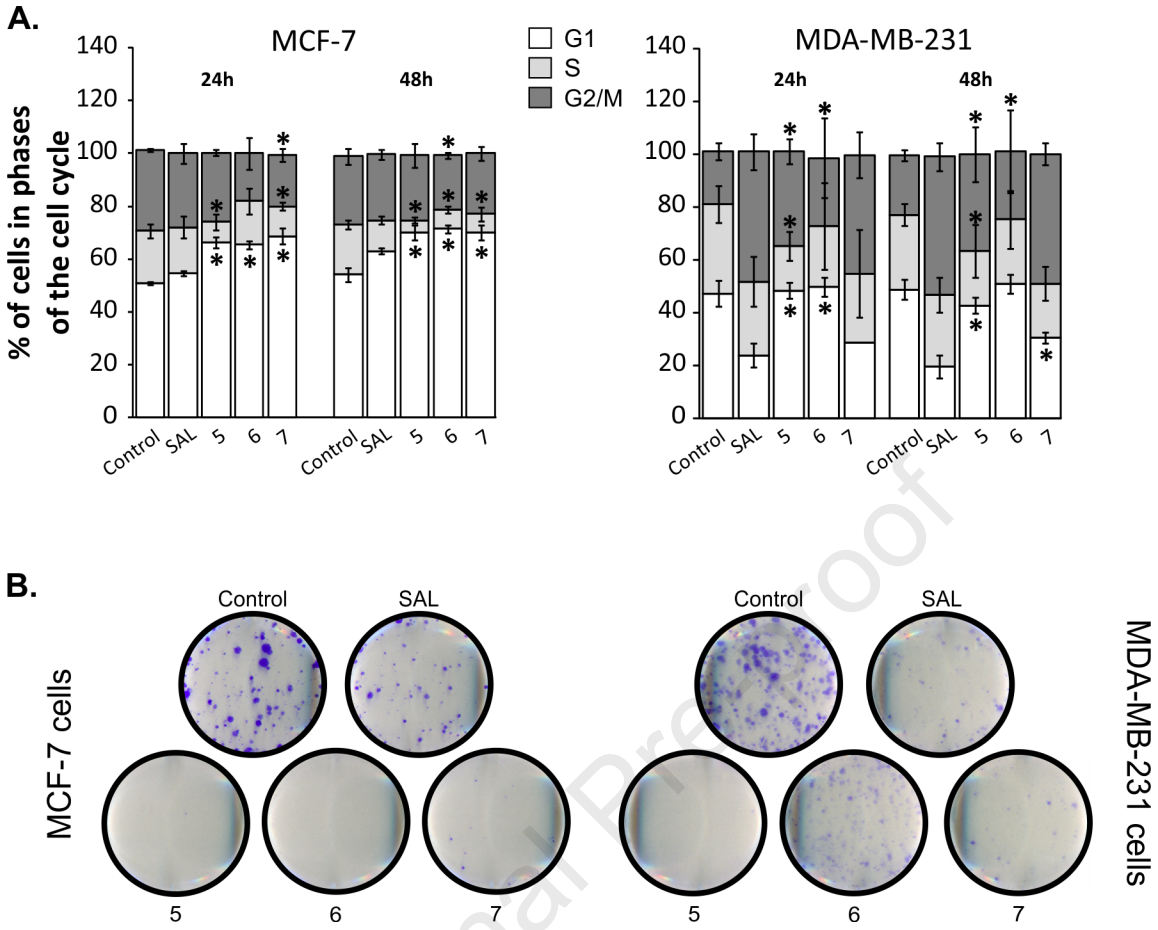

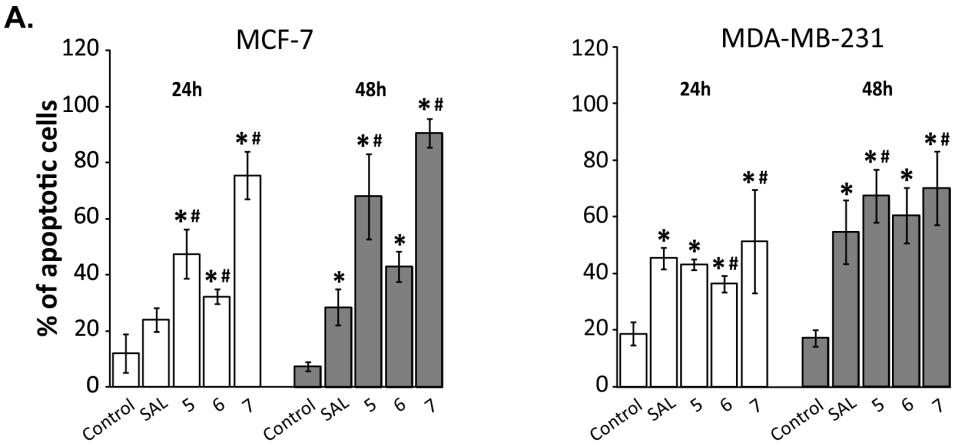
A.
MCF-7
MDA-MB-231
% of apoptotic cells
24h
48h
Control
SAL
5
6
7

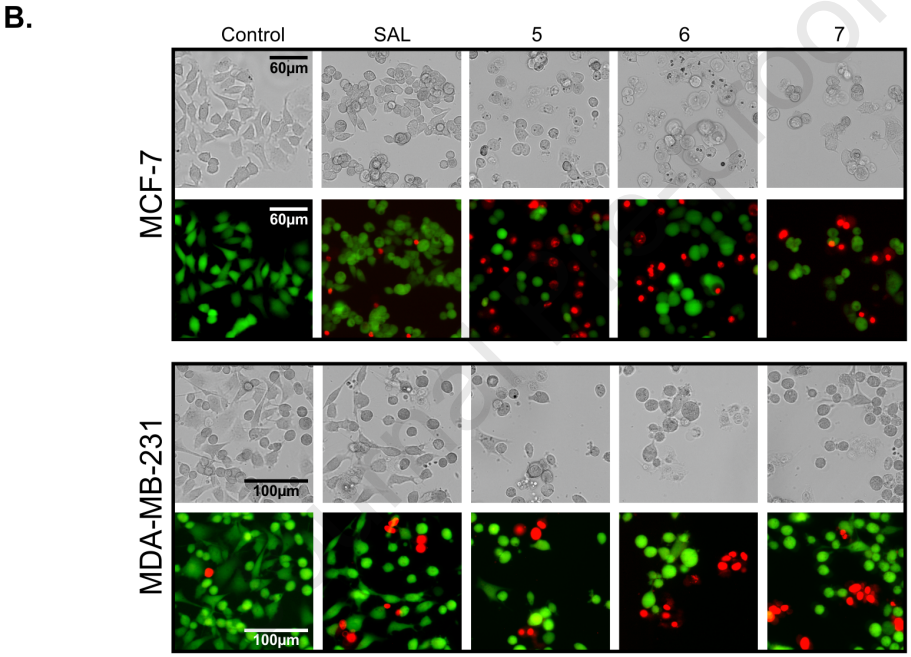
B.
Control
SAL
5
6
7
MCF-7
MDA-MB-231
60μm
100μm

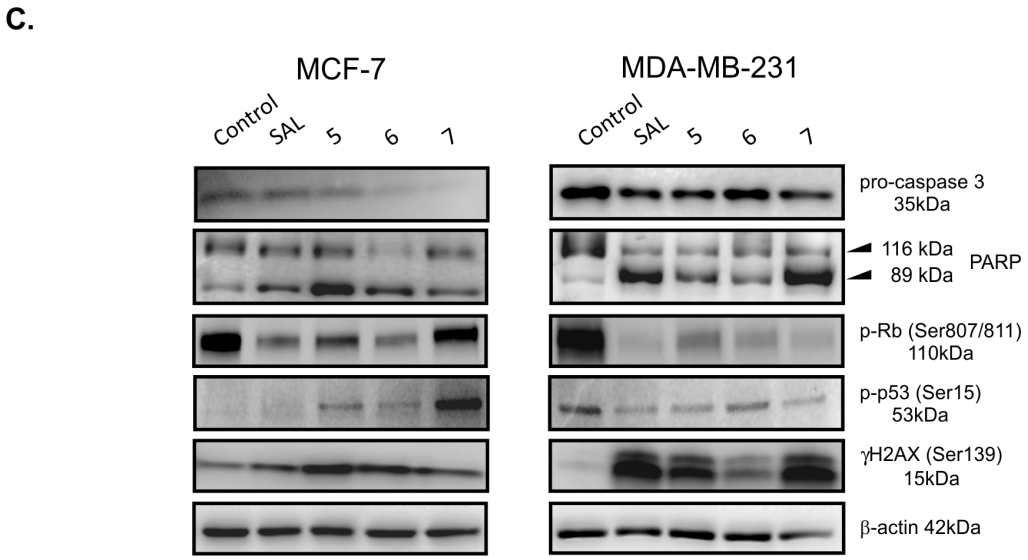
C.
MCF-7
MDA-MB-231
Control
SAL
5
6
7
pro-caspase 3
35kDa
116 kDa
89 kDa
PARP
p-Rb (Ser807/811)
110kDa
p-p53 (Ser15)
53kDa
γH2AX (Ser139)
15kDa
β-actin 42kDa

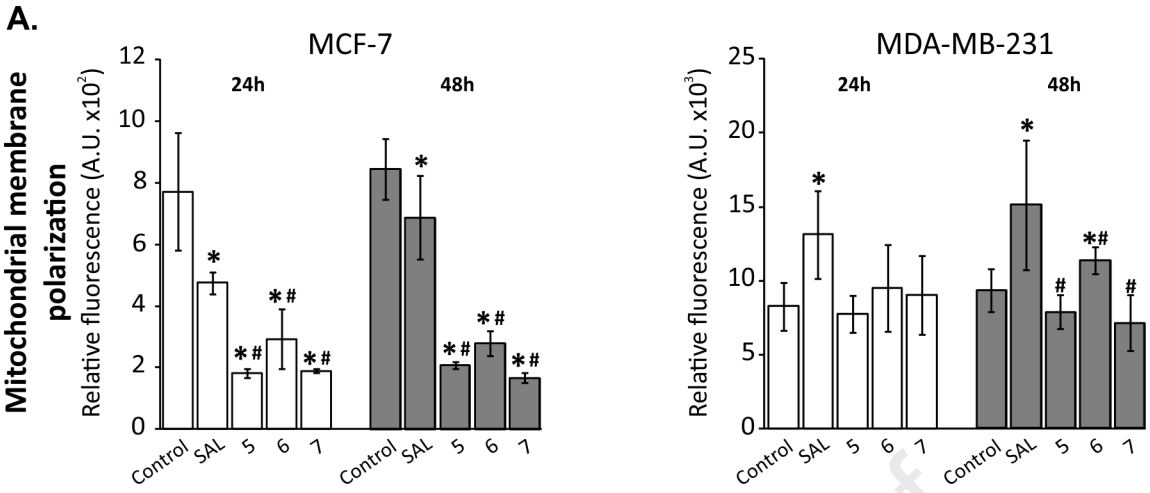

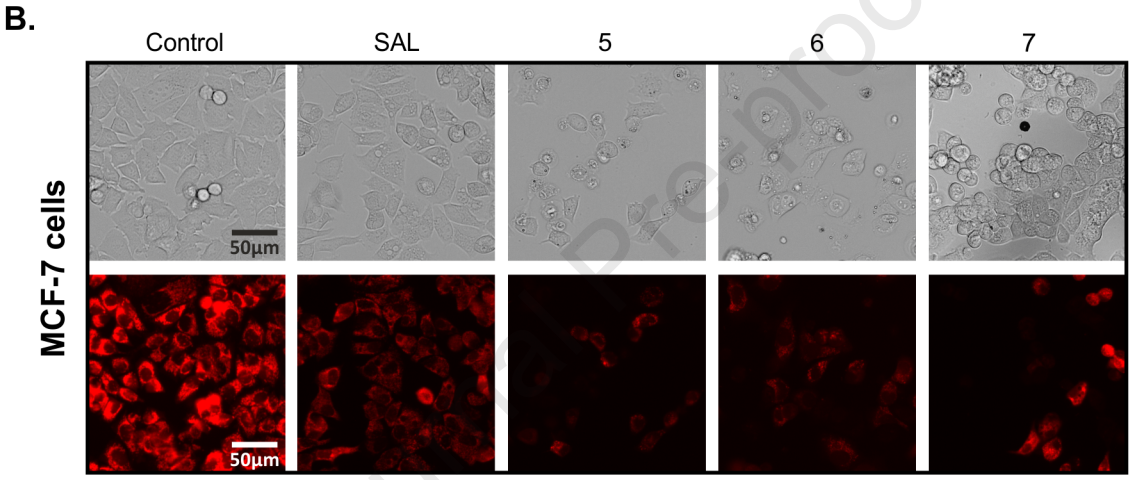

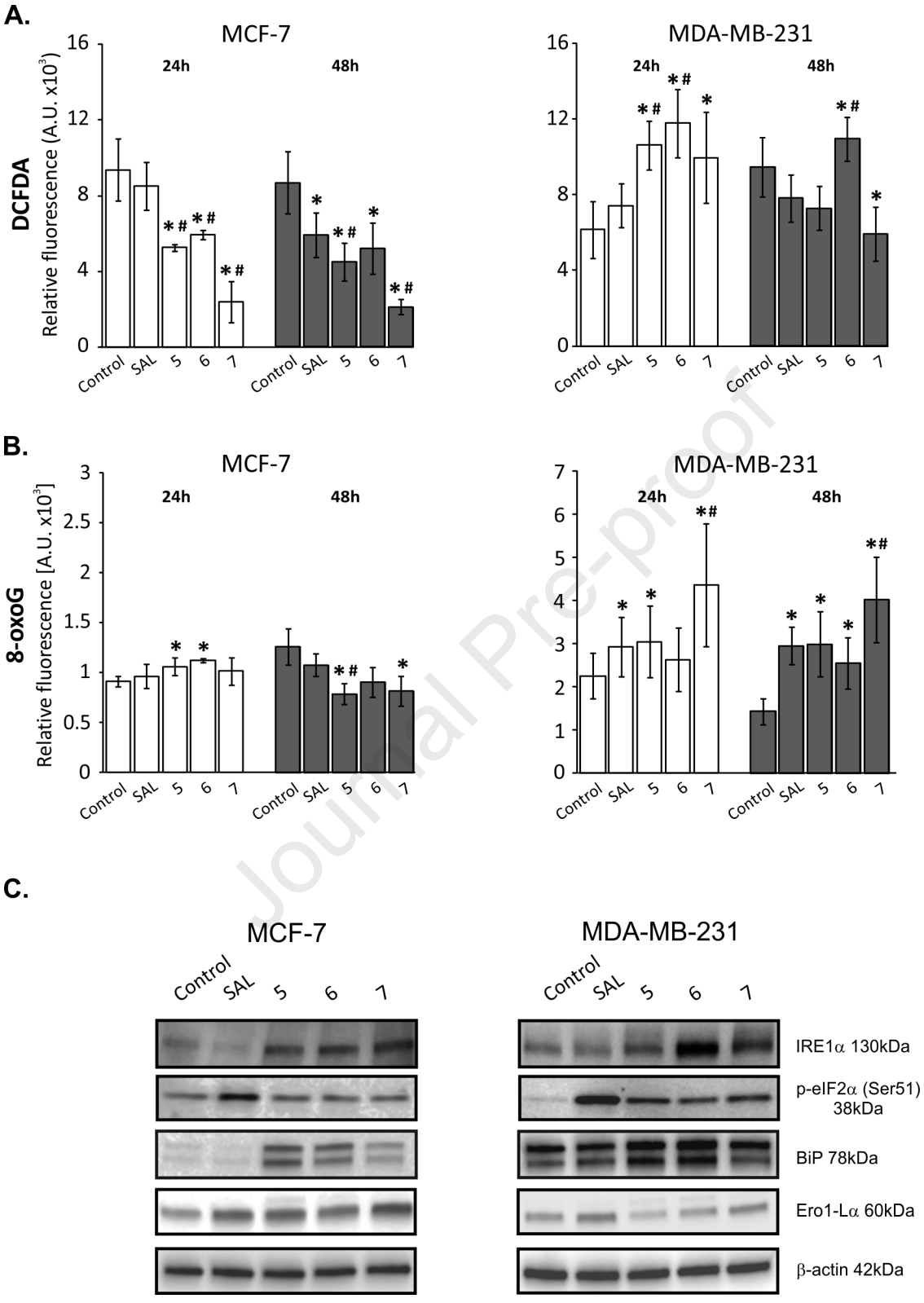

► Salinomycin and its ester and amide derivatives have been studied for anti-cancer activity.

► ER stress-induced apoptosis is the mechanism of action against MCF-7 and MDA-MB-231 cancer cells.

► When they are administered to the non-neoplastic normal breast fibroblasts displayed less toxicity.

► Salinomycin and its ester derivatives **5–7** increase the level of p-eIF2α (Ser51) and IRE1α proteins.